ChemPubSoc Europe

DOI: 10.1002/open.201600173

Open Access ChemistryOPEN Full Papers

Five-Component Self-Assembly of Cucurbituril-Based Hetero-pseudorotaxanes

Cátia Parente Carvalho[+],[a] Zoe Domínguez[+],[a] Cristina Domínguez,[a] Hamdy S. El-Sheshtawy,[b] José Paulo Da Silva,[c] Jesús F. Arteaga,[a] and Uwe Pischel*[a]

[5]Pseudorotaxanes can be obtained by self-sorting using heteroditopic guests and various cucurbituril homologues as hosts. The assembly and chemically induced disassembly of the pseudorotaxanes can be monitored by measuring the fluorescence of the anthracene guest in solution. Mass spectral evidence for the supramolecular assemblies is obtained in the gas phase. The disassembly in the gas phase can be achieved by collision-induced dissociation leading to the corresponding [2]- and [3]pseudorotaxanes.

1. Introduction

Self-assembly has received growing attention during recent years as a synthetic method for the construction of well-defined supramolecular architectures.[1–5] This interest is strongly driven by the desire to implement nature's recipes in artificial biomimetic systems and to obtain novel functional materials. The opportunities offered by the principles of self-sorting in combination with structurally and electronically pre-programmed building blocks have been demonstrated for the most diverse of systems.[4] Some of these systems make use of metal–ligand interactions,[6] whereas others embrace all-organic self-assembly.[5,7–10]

Cucurbiturils (CBs) are organic macrocycles that are composed of *n* glycoluril units linked by methylene bridges, where $n = 5$, 6, 7, 8, 10, and 14.[10–13] Recently, they have been in the focus of many research programs owing to their fascinating host–guest chemistry. Organic compounds with positively charged groups have been identified as preferred guests with association constants of up to 10^{15}–10^{17} M^{-1} in water, matching or even surpassing those of nature's strongest supramolecular assembly—the biotin–avidin pair.[14,15] The nanotechnological potential of CBs is currently being realized and spans from analytical applications, dye chemistry, materials chemistry, and supramolecular catalysis to topics inspired by the life sciences, such as biomolecule binding, drug delivery, and control of biological functions.[10,13,16–32] One central aspect of the chemistry of CBs is their role as prime components in self-sorting.[33–37] The variation of the cavity size of CB homologues and consequently the differentiation of the strength and dynamics of guest binding can trigger thermodynamically or kinetically driven selection processes.

Importantly, the extended set of available affinity data for CB6, CB7, and CB8 binding to structurally diverse guests[10,21,34,38] provides a solid foundation for the molecular design of complex supramolecular structures containing CB macrocycles as key elements. This might ultimately lead to complex, yet well-defined systems that exhibit biomimetic features.[10,28,33,35–37,39–41] In this study, we were especially interested in the use of CBs as wheel components of pseudorotaxanes. Previous reports (see Scheme 1) have often focused on two-component assemblies.[42–44] In an extension of these studies, multicomponent pseudorotaxanes were obtained through the complexation of CBs by a pre-programmed unimolecular axle.[36,37,39,40,45] However, the CB-templated assembly of homo[5]pseudorotaxanes by means of the formation of a 1:1:1 ternary complex that holds the axle components together, has only been scarcely reported (Scheme 1).[36,46]

In the present work, we made use of heteroditopic ligands that discriminate between CB homologues (CB6, CB7, and CB8) based on well-differentiated binding constants. The reasoned molecular design enabled the high-precision self-sorting of five components. This resulted, to the best of our knowledge, in unprecedented all-CB hetero[5]pseudorotaxanes with a self-assembled axle and different CB homologues as wheels

[a] Dr. C. P. Carvalho,[+] Z. Domínguez,[+] C. Domínguez, Dr. J. F. Arteaga, Dr. U. Pischel
CIQSO—Center for Research in Sustainable Chemistry and Department of Chemistry, University of Huelva
Campus de El Carmen, 21071 Huelva (Spain)
E-mail: uwe.pischel@diq.uhu.es

[b] Dr. H. S. El-Sheshtawy
Chemistry Department, Faculty of Science
Kafrelsheikh University
33516 Kafr ElSheikh (Egypt)

[c] Dr. J. P. D. Silva
Meditbio—Faculty of Sciences and Technology
University of Algarve
Campus de Gambelas, 8005-139 Faro (Portugal)

[+] These authors contributed equally to this work

Supporting Information and the ORCID identification number(s) for the author(s) of this article can be found under http://dx.doi.org/10.1002/open.201600173.

© 2017 The Authors. Published by Wiley-VCH Verlag GmbH & Co. KGaA. This is an open access article under the terms of the Creative Commons Attribution-NonCommercial-NoDerivs License, which permits use and distribution in any medium, provided the original work is properly cited, the use is non-commercial and no modifications or adaptations are made.

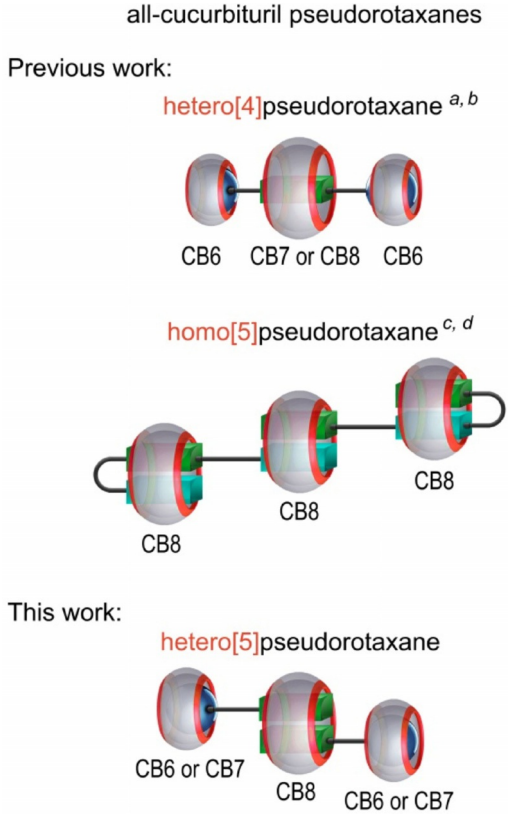

Scheme 1. Examples of all-CB pseudorotaxanes and representation of the target structures in this study. [a] Ref. [39]. [b] Ref. [40]. [c] Ref. [36]. [d] Ref. [46].

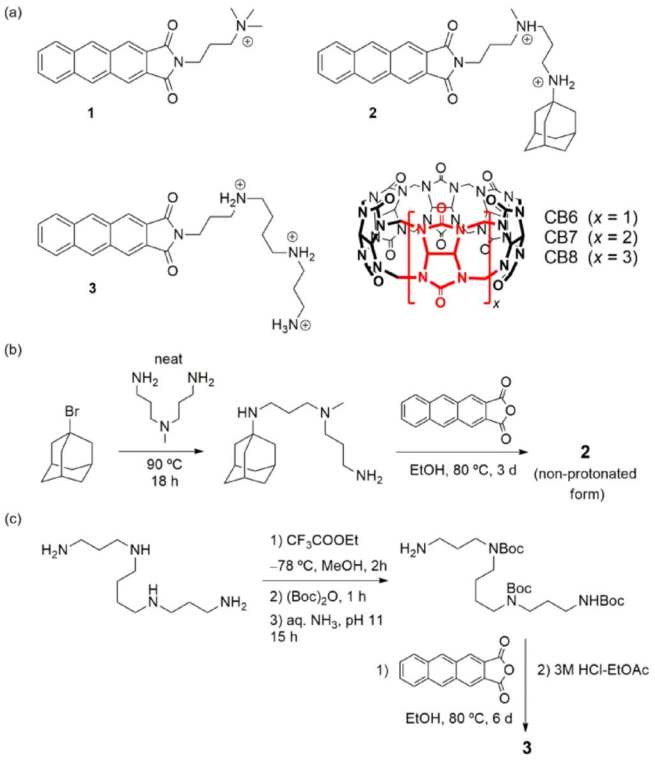

Scheme 2. a) Structures of the previously prepared anthracene-2,3-imide derivative **1** (Ref. [47]), compounds **2** and **3** in their fully protonated form, and the CBs used in this work. b) Synthesis of **2**. Note that compound **2** was obtained as a non-protonated amine after column chromatography under basic conditions (see the Experimental Section). c) Synthesis of **3**.

(Scheme 1). Likewise, using only CB8 yielded all-CB8 homo[5]-pseudorotaxanes. Furthermore, the molecular design included the possibility to monitor the supramolecular processes by fluorescence spectroscopy and electrospray ionization mass spectrometry (ESI-MS).

2. Results and Discussion

2.1. Molecular Design

Our approach makes use of the previously[47] observed strong 2:1 complexation of the model compound **1** (Scheme 2a) by CB8 ($K_{21}=4.2\times10^{12}\,\text{M}^{-2}$; corresponding to an apparent 1:1 binding constant of $2.0\times10^{6}\,\text{M}^{-1}$, although it is likely that the first anthracene is bound more weakly than the second). The 1:1 complex with CB7 is weaker by one order of magnitude ($K_{11}=3.0\times10^{5}\,\text{M}^{-1}$).[47] In this study, we designed and prepared the derivatives **2** and **3**, combining the same anthracene imide chromophore as in **1** with an additional motif for binding homologous CB macrocycles (Scheme 2a–c and the Experimental Section). On the one hand, the aminoadamantane unit in **2** is well known to form extraordinarily strong 1:1 complexes with CB7 and somewhat weaker complexes with CB8 ($K=4.2\times10^{12}\,\text{M}^{-1}$ with CB7 versus $8.2\times10^{8}\,\text{M}^{-1}$ with CB8).[34] On the other hand, the spermidine tail in **3** should enable efficient complexation of CB6 ($K=4.1\times10^{8}\,\text{M}^{-1}$).[38] Hence, we expected to gain access to hetero[5]pseudorotaxanes by self-sorting formation based on the differentiated complexation of **2** by CB7 and CB8 and of **3** by CB6 and CB8, featuring a central ternary 2:1 anthracene–CB8 complex (Scheme 1, bottom). Likewise, for both guests the formation of homo[5]pseudorotaxanes is predicted for the stoichiometric presence of only CB8. It was anticipated that the well-differentiated binding affinities would guarantee high precision with respect to the final assemblies, underlining a unique quality of CB host–guest chemistry.

Conveniently, the chromophoric and fluorescent nature of the anthracene-binding motif provides a handle for monitoring the axle assembly by UV/Vis absorption and fluorescence spectroscopies. In aqueous solution (pH 6–7) compounds **2** and **3** feature a typical long-wavelength UV/Vis absorption band with a maximum at 413 nm and significant fluorescence (**2**: $\lambda_{\text{fluo, max}}=496$ nm, $\Phi_{\text{fluo}}=0.52$, $\tau_{\text{fluo}}=6.75$ ns; **3**: $\lambda_{\text{fluo, max}}=497$ nm, $\Phi_{\text{fluo}}=0.53$, $\tau_{\text{fluo}}=6.91$ ns; see the red spectra in Figure 1 for **2**).[47] As a general observation, the inclusion of the anthracene in CB8 is signaled by a bathochromic shift of the long-wavelength UV/Vis absorption band (from 413 to 433 nm) and a pronounced fluorescence quenching (≈90%), accompanied by a redshift of the emission by approximately 30–35 nm (Figure 1).[48]

© 2017 The Authors. Published by Wiley-VCH Verlag GmbH & Co. KGaA, Weinheim

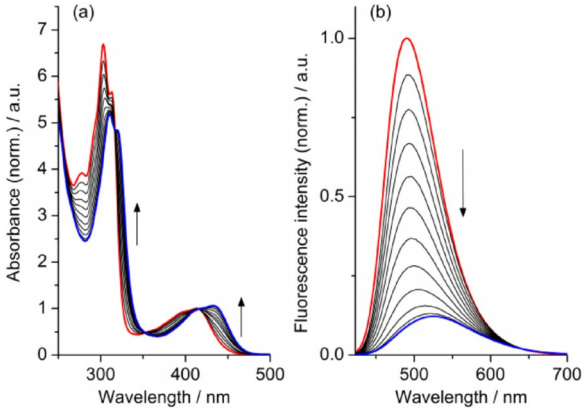

Figure 1. Titration of **2** (10 μM) with CB8 (0–19.7 μM) in water (pH 6); monitored by a) UV/Vis absorption and b) fluorescence (λ_{exc} = 419 nm). The initial and final spectra of the titration are colored red and blue, respectively. The initial spectra are normalized to 1 at the maximum of the longest-wavelength band.

2.2. Formation of [5]Pseudorotaxanes with Compound 2 and CB7/CB8 in Solution

In a first set of experiments, an aqueous solution (pH 6) of compound **2** was titrated with CB8 (Figure 2; black data points). The complexation proceeded in two well-defined phases. The addition of the first CB8 equivalent caused only a relatively small fluorescence quenching (≈24%), suggesting that mainly the aminoadamantane unit of **2** is bound along with a likely minor complexation of the anthracene unit (approximately two orders of magnitude higher binding constant with the adamantane than the apparent constant with the anthracene; see above). In a second phase, involving the addition of another 0.5 equivalents of CB8, the anthracene unit became visibly involved as indicated by the characteristic bathochromic shift of the absorption spectrum and a pronounced fluorescence quenching (≈90% at the titration endpoint; see Figure 1). This part of the titration corresponds to the dimerization of two 1:1 complexes (formed in the first stage), involving the CB8 complexation of two anthracene units. Hence, in total two molecules of **2** and three CB8 macrocycles interact, yielding the homo[5]pseudorotaxane $[(\mathbf{2})_2(CB8)_3]^{4+}$ (Scheme 1, bottom).[49]

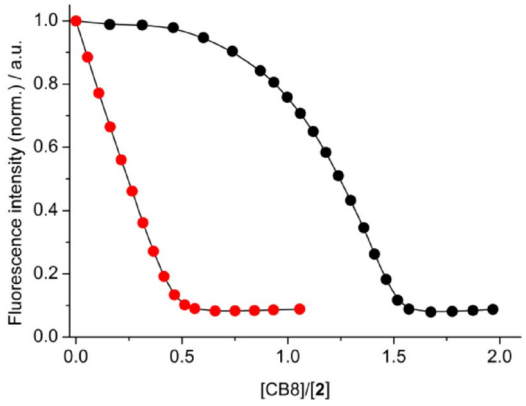

Figure 2. Fluorescence titration curves of **2** (10 μM) with CB8 (up to 19.7 μM) in water (pH 6, λ_{exc} = 419 nm, λ_{obs} = 490 nm) in the absence (black) and in the presence of CB7 (15 μM, red).

To take advantage of the binding characteristics of **2** toward CB7 and CB8, a similar experiment as described before, but with one equivalent CB7 present in the initial solution, was performed. The CB7 macrocycle binds four orders of magnitude stronger to the aminoadamantane unit than CB8 does (see above). Therefore, it was expected that the addition of CB8 would immediately induce the dimerization by complexation of two anthracene units with CB8. This was indeed the case, as experimentally corroborated by the changes in the optical signature, that is, fluorescence quenching and redshifted emission spectrum, and the sharp leveling off of the titration curve at 0.5 equivalents of CB8 (see Figure 2, red points). The supramolecular assembly corresponds to a hetero[5]pseudorotaxane $[(\mathbf{2})_2CB8(CB7)_2]^{4+}$ with a central CB8 and two terminal CB7 units (Scheme 1, bottom).

Also, the reverse titration, that is, addition of CB7 to a solution of **2** containing 0.5 equivalents of CB8, gave rise to a characteristic bathochromic UV/Vis absorption shift, indicative of the inclusion of the anthracene unit into CB8 (Figure 3). The titration curve shows a typical S shape. Initially, the CB7 binds readily to noncomplexed **2** because only 0.5 equivalents CB8 are present. Upon further titration, CB7 competes with CB8 for the aminoadamantane unit of **2** and the released CB8 associates to the available anthracene unit, yielding again the above-described hetero[5]pseudorotaxane. As expected for an equilibrium situation, the order of addition of the pseudorotaxane components was irrelevant for the outcome; exactly the same final spectral signature was obtained whether the order was **2**–CB7–CB8 or CB8–CB7–**2** (first–second–third). In general, the high uniformity of all complexation processes is underpinned by well-defined spectral changes and the occurrence of several isosbestic points in the UV/Vis absorption spectra.

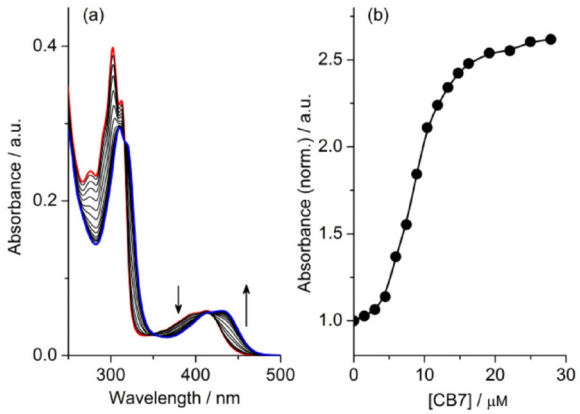

Figure 3. a) UV/Vis absorption titration of **2** (10 μM) with CB7 (0–27.8 μM) in the presence of CB8 (5 μM) in aqueous solution (pH 6). The red spectrum corresponds to the starting point, and the blue spectrum marks the endpoint of the titration. b) The corresponding titration curve, monitored at λ_{obs} = 435 nm.

© 2017 The Authors. Published by Wiley-VCH Verlag GmbH & Co. KGaA, Weinheim

By exploiting the reversible nature of host–guest complexation, it was of interest to demonstrate the disassembly of the pseudorotaxanes by means of the addition of a competitive guest for CB8. For this purpose, the sterically demanding aminoadamantane derivative memantine was used, which is known to form strong complexes with CB8 ($K = 4.3 \times 10^{11}\ M^{-1}$) but it binds much less efficiently to the smaller CB7 ($K = 2.5 \times 10^{4}\ M^{-1}$).[34] Titration of the [5]pseudorotaxanes $[(\mathbf{2})_2CB8(CB7)_2]^{4+}$ and $[(\mathbf{2})_2(CB8)_3]^{4+}$ with this competitor guest yielded the recovery of the initial UV/Vis absorption and fluorescence properties of the non-complexed anthracene chromophore (see the Supporting Information). These experiments showed that memantine can be used to disassemble the central 2:1 ternary CB8 complex, which is conveniently signaled by fluorescence enhancement.

2.3. Formation of [5]Pseudorotaxanes with Compound 2 in the Gas Phase

Solution titrations and monitoring of the changes of optical spectral features can provide information about the binding stoichiometry, and in combination with calculation of binding constants, allow for a reasoned discussion of the nature of the formed assemblies. However, it was highly desirable to draw on a complementary technique to corroborate our conclusions further. In the light of the limited CB8 solubility, which complicated the NMR spectroscopy experiments, ESI-MS was the analytical technique of choice for this work. The use of ESI-MS enabled an insightful analysis of the multicomponent mixtures in the micromolar concentration range (Figure 4).[36,37,50]

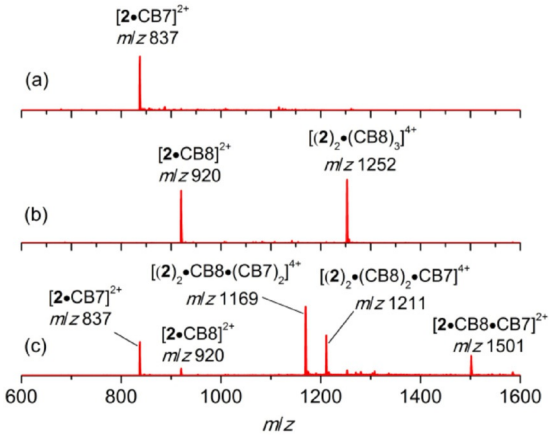

Figure 4. ESI-MS spectra of **2** (10 μM); a) with CB7 (10 μM), b) with CB8 (15 μM), c) with CB8 (5 μM) and CB7 (10 μM).

The ESI-MS spectrum of a 1:1 mixture of **2** and CB7 features one signal at *m/z* 837 (Figure 4a). The corresponding species was assigned as $[\mathbf{2}(CB7)]^{2+}$. The fragmentation (MS^2) of this ion yielded signals that can be attributed 1) to a CB7 complex containing an adamantyl-substituted fragment and 2) to an unbound anthracene-2,3-imide fragment. This finding provided support for the preferential binding of CB7 to the adamantane unit (see the MS^2 spectrum in the Supporting Information). The mass spectrum of a **2**/CB8 mixture (2:3) yielded clear evidence for the homo[5]pseudorotaxane (Figure 4b) discussed above. Specifically, two signals at *m/z* 920 and 1252 were detected and were assigned to the 1:1 complex $[\mathbf{2}(CB8)]^{2+}$ and the homo[5]pseudorotaxane $[(\mathbf{2})_2(CB8)_3]^{4+}$, respectively. Fragmentation (MS^2) of the latter ion gave the corresponding 1:1 complex $[\mathbf{2}(CB8)]^{2+}$ and the [3]pseudorotaxane $[\mathbf{2}(CB8)_2]^{2+}$, indicating preferential disassembly of the central 2:1 ternary CB8 complex. This is in accordance with the relative stabilities of the involved complexes (see above).

The mixture of **2**, CB7 and CB8 ([**2**]/[CB7]/[CB8] = 1:1:0.5) gave rise to a prevailing signal at *m/z* 1169, corresponding to the hetero[5]pseudorotaxane $[(\mathbf{2})_2CB8(CB7)_2]^{4+}$, and a signal at *m/z* 1211, assigned to $[(\mathbf{2})_2(CB8)_2CB7]^{4+}$ with one CB7 and one CB8 at the terminal positions (Figure 4c). As illustrated in Figure 5 (see the Supporting Information for the MS^2 spectra),

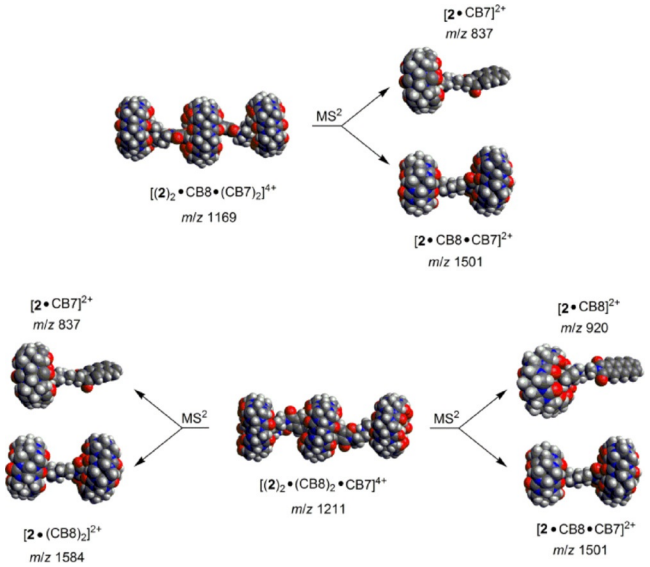

Figure 5. Principal MS^2 fragmentation products for the *m/z* 1169 and 1211 ions. The models correspond to MM2-optimized structures of the complexes. The corresponding MS^2 spectra are shown in the Supporting Information.

fragmentation of the *m/z* 1169 ion provided as the main signals those of $[\mathbf{2}(CB7)]^{2+}$ and $[\mathbf{2}(CB8)(CB7)]^{2+}$, again pointing to the disassembly of the central 2:1 ternary anthracene–CB8 complex (see the discussion above). Fragmentation of the *m/z* 1211 ion led to a more complex situation, derived from the unsymmetrical arrangement of different CB macrocycles at the terminal adamantane moieties. Specifically, $[\mathbf{2}(CB7)]^{2+}$ (*m/z* 837), $[\mathbf{2}(CB8)]^{2+}$ (*m/z* 920), $[\mathbf{2}(CB8)(CB7)]^{2+}$ (*m/z* 1501), and $[\mathbf{2}(CB8)_2]^{2+}$ (*m/z* 1585) were detected (see Figure 5 and the Supporting Information). Hence, the mass evidence, MS^2 fragmentation experiments, and the solution titrations provide clear support for the formation of [5]pseudorotaxanes containing the heteroditopic building block **2**.

© 2017 The Authors. Published by Wiley-VCH Verlag GmbH & Co. KGaA, Weinheim

2.4. Formation of a Hetero[5]pseudorotaxane with Compound 3 and CB6/CB8

Derivative **3** was designed to investigate the molecular diversity of the supramolecular five-component assembly of hetero[5]pseudorotaxanes, using CB6 and CB8 in this case. As outlined above, the spermidine tail of the anthracene-2,3-imide derivative **3** should provide an efficient binding motif for CB6, functioning as terminal macrocycles of the targeted hetero[5]-pseudorotaxane. As for **2**, the axle was expected to organize by the formation of a ternary complex between two anthracene moieties and a CB8 macrocycle.

First, compound **3** was titrated with CB8, with monitoring of the changes in the UV/Vis absorption and fluorescence spectra (Figure 6). Again, the typical spectral changes as noted for the

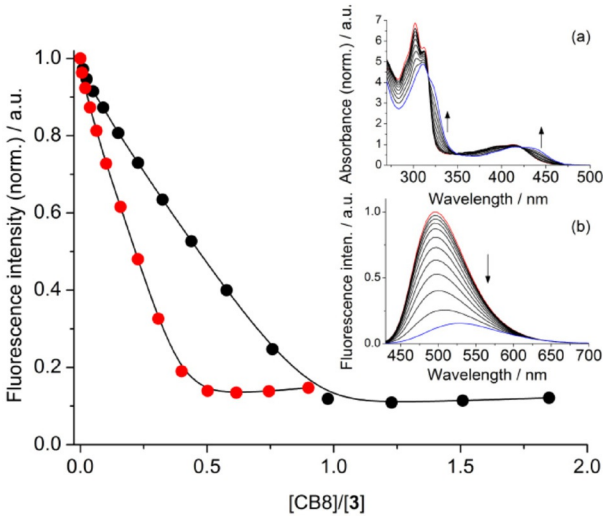

Figure 6. Fluorescence titration curves for the addition of CB8 (up to 9.2 μM) to **3** (5 μM) in the absence (black, λ_{obs} = 497 nm) and presence of CB6 (red, 11 μM, λ_{obs} = 490 nm) in water (pH 7). Inset: the development of the absorption spectra (a) and the fluorescence spectra (b) for the titration in the absence of CB6; initial and final spectra are colored red and blue, respectively. The initial spectra are normalized to 1 at the maximum of the longest-wavelength band.

case of guest **2** (see above) were observed.[48] Much to our initial surprise, and in contrast to the results that were obtained for **2**, no formation of a 2:1 ternary complex involving the anthracene unit could be concluded. Instead, the titration curve leveled off at approximately 1 equivalent CB8, indicating a 1:1 stoichiometry of the complex with the anthracene unit (Figure 6; black data points).

However, in the presence of 1 equivalent of CB6 in the initial solution, the titration reached its endpoint with approximately 0.5 equivalents of CB8 (Figure 6, red data points). Akin to the situation observed for **2** (using CB7), this result hints at the formation of a hetero[5]pseudorotaxane, in which the two CB6 macrocycles occupy the terminal spermidine chains of two molecules of **3** that are joined by a central CB8 in a 2:1 ternary complex (see the general representation in Scheme 1, bottom). Interestingly, it is the CB6 complexation that somewhat alleviates the coulombic repulsion between the highly charged spermidine tails, which promotes a positive cooperativity effect on the self-assembly of the desired hetero[5]pseudorotaxane.

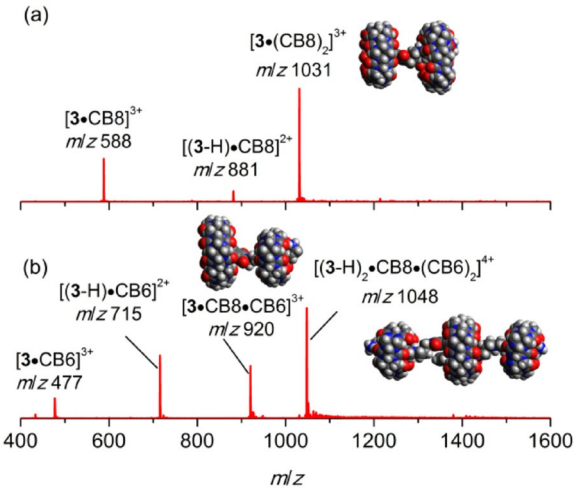

Figure 7. ESI-MS spectra of a) **3** (20 μM) with 1.5 equiv. CB8 (30 μM), and b) **3** (10 μM) in presence of 0.5 equiv. CB8 (5 μM) and 1 equiv. CB6 (10 μM); all in water (pH 7). The models of the detected [3]- and [5]pseudorotaxanes are also shown.

The gas-phase ESI-MS studies (Figure 7) confirmed the formation of the pseudorotaxanes. In the presence of CB8, the [3]pseudorotaxane with the fully protonated axle **3** was observed, $[\mathbf{3}(CB8)_2]^{3+}$ at *m/z* 1031. However, most of **3** is integrated in [2]pseudorotaxanes with varying charge status, that is, $[\mathbf{3}(CB8)]^{3+}$ (*m/z* 588) and $[(\mathbf{3}\text{-H})CB8]^{2+}$ (*m/z* 881). Contrary to the observations made for **2**, the homo[5]pseudorotaxane composed of two molecules of **3** and three of CB8 was not observed, which is consistent with the solution studies.

In the presence of both CB6 and CB8 ([**3**]/[CB6]/[CB8] = 1:1:0.5), the predicted hetero[5]pseudorotaxane $[(\mathbf{3}\text{-H})_2CB8(CB6)_2]^{4+}$ was most abundant, as indicated by a dominant signal at *m/z* 1048. Other less abundant species were the [2]- and [3]pseudorotaxanes $[(\mathbf{3}\text{-H})CB6]^{2+}$ and $[\mathbf{3}(CB8)(CB6)]^{3+}$ corresponding to signals at *m/z* 715 and 920, respectively. The MS^2 fragmentation of the hetero[5]pseudorotaxane showed the collision-induced dissociation into the corresponding fragments: $[(\mathbf{3}\text{-H})CB6]^{2+}$ and $[(\mathbf{3}\text{-H})CB8(CB6)]^{2+}$ (see the Supporting Information). These observations are akin to the gas-phase chemistry of the [5]pseudorotaxanes based on compound **2**, confirming the preferential dissociation of the central 2:1 ternary CB8 complex.

3. Conclusions

Heteroditopic fluorescent guests with high and well-differentiated binding constants for cucurbiturils (CB6, CB7, CB8) as well as variable complex stoichiometries (2:1 vs. 1:1) can be used for the controlled self-assembly of all-CB homo- and hetero[5]-pseudorotaxanes. This study underpins the unique strength of cucurbiturils as components in programmed self-sorting processes that lead to complex supramolecular structures that

© 2017 The Authors. Published by Wiley-VCH Verlag GmbH & Co. KGaA, Weinheim

might have applications as biomimetic materials. Furthermore, the tailored formation of the pseudorotaxanes can be monitored by optical spectroscopy, providing another functional facet to the molecular design of the axle building blocks.

Experimental Section

Materials

All reagents and solvents for synthesis were commercially available (Sigma–Aldrich) in high purities and used as received. Water was of Milli-Q quality. CB7 was synthesized according to a previously published procedure,[51] whereas CB6 and CB8 were purchased from Sigma–Aldrich. N^1,N^5,N^{10}-Tri-Boc-spermine was prepared according to a literature procedure.[52]

Synthesis of Compound 2

1-Bromoadamantane (2.00 g, 9.30 mmol) and 3,3′-diamino-*N*-methyldipropylamine (6.75 g, 46.5 mmol) were mixed in a sealed tube. This mixture was heated at 190 °C for 20 h. The mixture was allowed to cool to room temperature, then HCl (2 M, 60 mL) and diethyl ether (60 mL) were added. The aqueous phase was separated and 50% NaOH solution (60 mL) was added. Finally, the product was extracted with diethyl ether (3×40 mL) and the combined organic phases were dried with anhydrous Na_2SO_4. Removal of the solvent gave N^1-(adamantan-1-yl)-N^3-(3-aminopropyl)-N^3-methylpropane-1,3-diamine as an oil (1.71 g, 66% yield). This material was used in the next step without further purification.

2,3-Anthracenedicarboxylic anhydride (60 mg, 0.24 mmol), N^1-(adamantan-1-yl)-N^3-(3-aminopropyl)-N^3-methyl-propane-1,3-diamine (67.5 mg, 0.24 mmol), and triethylamine (51 μL, 0.37 mmol) were placed together with ethanol (5 mL) in a sealed tube. This mixture was heated at 80 °C for 72 h. Afterwards, all volatiles were removed and the residue was subjected to column chromatography on silica gel (CH_2Cl_2/CH_3OH/NH_4OH, 50:10:1). Compound **2**, in its non-protonated form, was isolated as a solid (35 mg, 28% yield).

N^1-(Adamantan-1-yl)-N^3-(3-aminopropyl)-N^3-methylpropane-1,3-diamine: ^{1}H NMR (400 MHz, $CDCl_3$): $\delta = 2.62$ (t, $J = 7.2$ Hz, 2H), 2.49 (t, $J = 7.2$ Hz, 2H), 2.26 (t, $J = 7.2$ Hz, 4H), 2.09 (s, 3H), 1.95 (br s, 3H), 1.60–1.44 (m, 16H), 1.01 ppm (br s, 3H); ^{13}C NMR (100 MHz, $CDCl_3$): $\delta = 56.3$, 55.5, 50.2, 42.7, 42.3, 40.7, 39.0, 36.7, 31.2, 29.5, 28.6 ppm; HRMS (ESI): *m/z*: calcd for $C_{17}H_{34}N_3$: 280.2747 $[M+H]^+$; found: 280.2746.

Compound **2**: ^{1}H NMR (400 MHz, $CDCl_3$): $\delta = 8.52$ (s, 2H), 8.39 (s, 2H), 8.04–7.98 (m, 2H), 7.60–7.54 (m, 2H), 3.77 (t, $J = 7.2$ Hz, 2H), 2.62 (t, $J = 7.2$ Hz, 2H), 2.43 (t, $J = 7.2$ Hz, 2H), 2.38 (t, $J = 7.2$ Hz, 2H), 2.20 (s, 3H), 2.03 (br s, 3H), 1.94–1.82 (m, 2H), 1.69–1.52 ppm (m, 14H); the NH shows as a broad signal at approximately 2.6 ppm; ^{13}C NMR (100 MHz, $CDCl_3$): $\delta = 167.9$, 133.2, 131.9, 130.0, 128.5, 127.5, 126.6, 125.7, 56.4, 55.3, 51.0, 42.3, 42.0, 39.2, 36.7, 36.6, 29.6, 27.9, 26.3 ppm; HRMS (ESI): *m/z*: calcd for $C_{33}H_{40}N_3O_2$: 510.3115 $[M+H]^+$; found: 510.3111.

Synthesis of Compound 3

N^1,N^5,N^{10}-Tri-Boc-spermine (140 mg, 0.28 mmol), triethylamine (39 μL, 0.28 mmol), and ethanol (5 mL) were placed in a sealed tube and the solution was stirred for 15 min. Then, 2,3-anthracenedicarboxylic anhydride (69.1 mg, 0.28 mmol) was added slowly and the resulting mixture was heated to 80 °C for 6 days. The mixture was allowed to cool to room temperature, then the volatiles were removed and the residue was subjected to column chromatography on silica gel (CH_2Cl_2/MeOH/NH_4OH, 50:10:1). The product was obtained as a solid (148 mg, 72% yield) and used directly in the next step without further characterization. A portion of this material (99 mg, 0.14 mmol) was treated with HCl (3 M) in ethyl acetate (1 mL) in a round-bottom flask. After the reaction was stirred for 90 min at room temperature the volatiles were evaporated to give compound **3**, which was assumed to be the trihydrochloride salt (50 mg, 68% yield). ^{1}H NMR (400 MHz, D_2O): $\delta = 7.56$ (s, 2H), 7.52–7.45 (m, 2H), 7.32–7.26 (m, 2H), 7.20 (s, 2H), 3.42 (t, $J = 7.2$ Hz, 2H), 3.18–3.00 (m, 10H), 2.13–2.02 (m, 2H), 2.00–1.89 (m, 2H), 1.85–1.70 ppm (m, 4H); ^{13}C NMR (100 MHz, CD_3OD): $\delta = 170.3$, 133.7, 131.8, 131.2, 129.4, 128.6, 127.4, 125.3, 48.0, 47.9, 46.2, 45.5, 37.5, 35.9, 25.8, 24.8, 23.8 ppm (2×); HRMS (ESI): *m/z*: calcd for $C_{26}H_{33}N_4O_2$: 433.2598 $[M-2H]^+$; found: 433.2595.

Photophysical Measurements and Titrations

All measurements were performed with air-equilibrated water solutions at room temperature, using quartz cuvettes (1 cm optical pathlength). Compound **2** was pre-solubilized in DMSO and the final aqueous solutions (pH 6) contained 1 vol% of the organic co-solvent. Compound **3** was sufficiently soluble in water (pH 7). The UV/Vis absorption spectra were measured with a UV-1603 spectrophotometer (Shimadzu). Steady-state fluorescence spectra (uncorrected) were measured on a Cary Eclipse fluorimeter (Varian). The fluorescence quantum yield was measured for corrected emission spectra, with quinine sulfate in 0.05 M H_2SO_4 as a reference ($\Phi_{fluo} = 0.55$).[53,54] The fluorescence lifetimes were determined by time-correlated single-photon counting (Edinburgh Instruments FLS 920).

Titration experiments were performed by adding aliquots of CB stock solutions. These were accompanied by the same concentration of the guest compound as present in the titrated solution, thereby avoiding dilution effects in the course of the experiment. Isosbestic points of the UV/Vis absorption titration were selected as excitation wavelengths for fluorescence titrations. If required, the pH was adjusted by the addition of dilute aqueous HCl or NaOH and kept constant during the titrations. The concentration of the CB8 stock solution was determined by titration with *N*,*N*-dimethylaminophenyltropyilium perchlorate.[55] CB7 was assumed to have 14 wt% water content (determined by ^{1}H NMR spectroscopy in the presence of malonic acid as an internal standard). The water content of CB6 was indicated by the supplier to be 25 wt%.

Electrospray Ionization Mass Spectrometry

The electrospray ionization (ESI) mass spectra were obtained using a Bruker Esquire HCT ultra ion-trap mass spectrometer, equipped with an ESI source (Agilent). The solutions of the compounds were infused into the ESI source at a rate of 4 μL min^{-1} with the aid of a syringe pump (KdScientific, model 781100, Holliston, MA, USA). Typical spray and ion optics conditions were as follows: capillary voltage, 3.0 kV; nebulizer gas pressure, 30 psi; drying gas temperature, 300 °C; drying gas flow, 6 L min^{-1}; capillary exit voltage, 179 V; skimmer voltage, 30 V. The charge status of the detected ions was determined from the isotope spacing patterns.

Molecular Modeling of the Pseudorotaxanes

Modeling was performed using the ChemOffice software package (version 8). The structures of the free CB macrocycles (CB7 and

 © 2017 The Authors. Published by Wiley-VCH Verlag GmbH & Co. KGaA, Weinheim

CB8) correspond to their crystal structures[56,57] and the guests **2** or **3** were connected to the macrocycle with the Avogadro software (version 1.1.1). The structures were optimized by molecular mechanics minimization (MM2 force field), using the ChemBio3D Ultra software (version 8).

Acknowledgements

We acknowledge the financial support of the Ministerio de Economía y Competitividad, Madrid, Spain (grants CTQ2011-28390 and CTQ2014-54729-C2-1-P for U.P. and PhD fellowship BES-2015–074458 for Z.D.), the Junta de Andalucía (grant P12-FQM-2140 for U.P.), and the Fundação para a Ciência e a Tecnologia, Lisbon, Portugal (grant SFRH/BD/81628/2011 for C.P.C.). H.S.E.-S. is grateful for a postdoctoral stipend from the Egyptian Ministry of Higher Education, Cairo.

Conflict of Interest

The authors declare no conflict of interest.

Keywords: fluorescence · host–guest systems · macrocycles · mass spectrometry · rotaxanes

[1] A. Wu, L. Isaacs, *J. Am. Chem. Soc.* **2003**, *125*, 4831.
[2] D. Ajami, J.-L. Hou, T. J. Dale, E. Barrett, J. Rebek, Jr., *Proc. Natl. Acad. Sci. USA* **2009**, *106*, 10430.
[3] W. Jiang, C. A. Schalley, *Proc. Natl. Acad. Sci. USA* **2009**, *106*, 10425.
[4] M. M. Safont-Sempere, G. Fernández, F. Würthner, *Chem. Rev.* **2011**, *111*, 5784.
[5] Z. He, W. Jiang, C. A. Schalley, *Chem. Soc. Rev.* **2015**, *44*, 779.
[6] R. Joseph, A. Nkrumah, R. J. Clark, E. Masson, *J. Am. Chem. Soc.* **2014**, *136*, 6602.
[7] E. S. Barrett, T. J. Dale, J. Rebek, Jr., *J. Am. Chem. Soc.* **2008**, *130*, 2344.
[8] Y. Rudzevich, V. Rudzevich, F. Klautzsch, C. A. Schalley, V. Böhmer, *Angew. Chem. Int. Ed.* **2009**, *48*, 3867; *Angew. Chem.* **2009**, *121*, 3925.
[9] M. Chas, G. Gil-Ramírez, E. C. Escudero-Adán, J. Bene *t*Buchholz, P. Ballester, *Org. Lett.* **2010**, 12, 1740.
[10] S. J. Barrow, S. Kasera, M. J. Rowland, J. del Barrio, O. A. Scherman, *Chem. Rev.* **2015**, *115*, 12320.
[11] J. Lagona, P. Mukhopadhyay, S. Chakrabarti, L. Isaacs, *Angew. Chem. Int. Ed.* **2005**, *44*, 4844; *Angew. Chem.* **2005**, *117*, 4922.
[12] E. Masson, X. Ling, R. Joseph, L. Kyeremeh-Mensah, X. Lu, *RSC Adv.* **2012**, *2*, 1213.
[13] K. I. Assaf, W. M. Nau, *Chem. Soc. Rev.* **2015**, *44*, 394.
[14] M. V. Rekharsky, T. Mori, C. Yang, Y. H. Ko, N. Selvapalam, H. Kim, D. Sobransingh, A. E. Kaifer, S. Liu, L. Isaacs, W. Chen, S. Moghaddam, M. K. Gilson, K. Kim, Y. Inoue, *Proc. Natl. Acad. Sci. USA* **2007**, *104*, 20737.
[15] L. Cao, M. Šekutor, P. Y. Zavalij, K. Mlinarić-Majerski, R. Glaser, L. Isaacs, *Angew. Chem. Int. Ed.* **2014**, *53*, 988; *Angew. Chem.* **2014**, *126*, 1006.
[16] N. J. Wheate, A. I. Day, R. J. Blanch, A. P. Arnold, C. Cullinane, J. G. Collins, *Chem. Commun.* **2004**, 1424.
[17] A. Hennig, H. Bakirci, W. M. Nau, *Nat. Methods* **2007**, *4*, 629.
[18] A. R. Kennedy, A. J. Florence, F. J. McInnes, N. J. Wheate, *Dalton Trans.* **2009**, 7695.
[19] V. D. Uzunova, C. Cullinane, K. Brix, W. M. Nau, A. I. Day, *Org. Biomol. Chem.* **2010**, *8*, 2037.
[20] S. Ghosh, L. Isaacs, *J. Am. Chem. Soc.* **2010**, *132*, 4445.
[21] R. N. Dsouza, U. Pischel, W. M. Nau, *Chem. Rev.* **2011**, *111*, 7941.
[22] J. M. Chinai, A. B. Taylor, L. M. Ryno, N. D. Hargreaves, C. A. Morris, P. J. Hart, A. R. Urbach, *J. Am. Chem. Soc.* **2011**, *133*, 8810.
[23] F. Tian, D. Jiao, F. Biedermann, O. A. Scherman, *Nat. Commun.* **2012**, *3*, 1207.
[24] D. Ma, G. Hettiarachchi, D. Nguyen, B. Zhang, J. B. Wittenberg, P. Y. Zavalij, V. Briken, L. Isaacs, *Nat. Chem.* **2012**, *4*, 503.
[25] B. C. Pemberton, R. Raghunathan, S. Volla, J. Sivaguru, *Chem. Eur. J.* **2012**, *18*, 12178.
[26] Y. Ahn, Y. Jang, N. Selvapalam, G. Yun, K. Kim, *Angew. Chem. Int. Ed.* **2013**, *52*, 3140; *Angew. Chem.* **2013**, *125*, 3222.
[27] L. A. Logsdon, A. R. Urbach, *J. Am. Chem. Soc.* **2013**, *135*, 11414.
[28] Z. Huang, L. Yang, Y. Liu, Z. Wang, O. A. Scherman, X. Zhang, *Angew. Chem. Int. Ed.* **2014**, *53*, 5351; *Angew. Chem.* **2014**, *126*, 5455.
[29] J. P. Da Silva, R. Choudhury, M. Porel, U. Pischel, S. Jockusch, P. C. Hubbard, V. Ramamurthy, A. V. M. Canário, *ACS Chem. Biol.* **2014**, *9*, 1432.
[30] F. Biedermann, W. M. Nau, *Angew. Chem. Int. Ed.* **2014**, *53*, 5694; *Angew. Chem.* **2014**, *126*, 5802.
[31] N. Basílio, U. Pischel, *Chem. Eur. J.* **2016**, *22*, 15208.
[32] J. Vázquez, M. A. Romero, R. N. Dsouza, U. Pischel, *Chem. Commun.* **2016**, *52*, 6245.
[33] P. Mukhopadhyay, A. Wu, L. Isaacs, *J. Org. Chem.* **2004**, *69*, 6157.
[34] S. Liu, C. Ruspic, P. Mukhopadhyay, S. Chakrabarti, P. Y. Zavalij, L. Isaacs, *J. Am. Chem. Soc.* **2005**, *127*, 15959.
[35] P. Mukhopadhyay, P. Y. Zavalij, L. Isaacs, *J. Am. Chem. Soc.* **2006**, *128*, 14093.
[36] W. Jiang, Q. Wang, I. Linder, F. Klautzsch, C. A. Schalley, *Chem. Eur. J.* **2011**, *17*, 2344.
[37] L. Cera, C. A. Schalley, *Chem. Sci.* **2014**, *5*, 2560.
[38] M. V. Rekharsky, Y. H. Ko, N. Selvapalam, K. Kim, Y. Inoue, *Supramol. Chem.* **2007**, *19*, 39.
[39] G. Celtek, M. Artar, O. A. Scherman, D. Tuncel, *Chem. Eur. J.* **2009**, *15*, 10360.
[40] E. Masson, X. Lu, X. Ling, D. L. Patchell, *Org. Lett.* **2009**, *11*, 3798.
[41] Q. Zhang, H. Tian, *Angew. Chem. Int. Ed.* **2014**, *53*, 10582; *Angew. Chem.* **2014**, *126*, 10754.
[42] V. Sindelar, K. Moon, A. E. Kaifer, *Org. Lett.* **2004**, *6*, 2665.
[43] V. Sindelar, S. Silvi, S. E. Parker, D. Sobransingh, A. E. Kaifer, *Adv. Funct. Mater.* **2007**, *17*, 694.
[44] V. Ramalingam, A. R. Urbach, *Org. Lett.* **2011**, *13*, 4898.
[45] P. Branná, M. Rouchal, Z. Prucková, L. Dastychová, R. Lenobel, T. Pospíšil, K. Maláč, R. Vícha, *Chem. Eur. J.* **2015**, *21*, 11712.
[46] Z.-J. Zhang, H.-Y. Zhang, L. Chen, Y. Liu, *J. Org. Chem.* **2011**, *76*, 8270.
[47] C. Parente Carvalho, Z. Domínguez, J. P. Da Silva, U. Pischel, *Chem. Commun.* **2015**, *51*, 2698.
[48] The fluorescence quenching is presumed to be due to the combination of environmental effects exerted by the CB8 cavity and π–π interactions between the guests in the case of ternary complex formation.
[49] Interestingly, the different pseudorotaxanes conferred a protective surrounding against chemical degradation of the guests **2** and **3**. Over the course of 5 h, less than 4% decomposition (monitored by UV/Vis absorption spectroscopy) was observed in all cases. This is in contrast with the moderate stability of free **2** and **3**, presumably provoked by a hydrolytic ring-opening of the imide (19% and 28% decomposition after 5 h for **2** and **3**, respectively).
[50] W. Jiang, A. Schäfer, P. C. Mohr, C. A. Schalley, *J. Am. Chem. Soc.* **2010**, *132*, 2309.
[51] C. Márquez, F. Huang, W. M. Nau, *IEEE Trans. Nanobiosci.* **2004**, *3*, 39.
[52] I. S. Blagbrough, A. J. Geall, *Tetrahedron Lett.* **1998**, *39*, 439.
[53] W. H. Melhuish, *J. Phys. Chem.* **1960**, *64*, 762.
[54] W. H. Melhuish, *J. Phys. Chem.* **1961**, *65*, 229.
[55] J. Vázquez, P. Remón, R. N. Dsouza, A. I. Lazar, J. F. Arteaga, W. M. Nau, U. Pischel, *Chem. Eur. J.* **2014**, *20*, 9897.
[56] A. L. Koner, C. Márquez, M. H. Dickman, W. M. Nau, *Angew. Chem. Int. Ed.* **2011**, *50*, 545; *Angew. Chem.* **2011**, *123*, 567.
[57] M. V. S. N. Maddipatla, M. Pattabiraman, A. Natarajan, K. Srivastav, J. T. Mague, V. Ramamurthy, *Org. Biomol. Chem.* **2012**, *10*, 9219.

Received: December 27, 2016
Published online on March 10, 2017

 © 2017 The Authors. Published by Wiley-VCH Verlag GmbH & Co. KGaA, Weinheim